Original Research Paper

IJES *Iranian Journal of Earth Sciences*
Vol. 13, No. 4, 2021, 288-298.
DOI: 10.30495/ijes.2021.685399

Identification of geochemical distribution of REEs using Factor Analysis and Concentration-Number (C-N) Fractal modeling in Granitoids, South of Varcheh 1:100000 sheet, Central Iran

Davoud Pirdadeh Beyranvand[1], Afshin Ashja Ardalan[1*], Taher Farhadinejad[2], Mohammad Ali Arian[1]

1. Department of Geology, North Tehran Branch, Islamic Azad University, Tehran, Iran
2. Soil Conservation and Watershed Management Research Department, Lorestan Agricultural and Natural Resources Research and Education Center, AREEO, Khoramabad, Iran

Received 12 December 2020; accepted 4 March 2021

Abstract

The purpose of the present research is delineating geochemical anomaly of REEs in granitoids in south of Varcheh 1:100,000 sheet by the use of C-N fractal model and classical statistical methods. We gathered and studied 59 rock samples for REEs by ICP-MS method in the laboratory of Iran Mineral Processing Research Center (IMPRC). The Concentration–Number (C-N) fractal model was used to delineate elemental thresholds. According to the results, the distribution of elemental concentration for Pr and Sm were divided to three classifications and Ce, La, Nd and Y had five geochemical populations in the area. The classical statistics methods were able to separate three geochemical populations. The results obtained by this study showed that the separation of geochemical anomalies for REEs using C-N fractal model and classical statistics methods yielded to the same results. Meanwhile, the high ratio of LREE to HREE in rock samples as well as high P content, assigns monazite, apatite, and sphene as a possible source of REEs in the study area.
Keywords: *Concentration-Number (C-N) Fractal Modeling, Factor Analysis, REEs, Varcheh*

1. Introduction

Segregate different geochemical anomalies from the background is crucial in the identification of ore-forming processes (Webb and Hawkes 1979; Carranza 2008; Afzal et al. 2013). Geochemical data analysis has been frequently used in the determination of thresholds and discrimination of different anomalies of elements (Rantitsch 2000; Pazand et al. 2011; Zuo 2011a; Zuo 2011b). Several methods such as conventional statistics and fractal models have been proposed for distinguishing geochemical anomalies from the background. Statistical analysis widely applied to separate geochemical anomalies based on different parameters such as the histogram analysis, summation of mean, standard deviation, and box plot (Davis 2002; Li et al. 2003; Carranza 2009; Arias et al. 2012; Daneshvar-Saein 2017). The application of the classic statistical techniques is satisfactory in a dataset in which a normal distribution is revealed and is composed of independent variables (Asadi et al. 2014). Since the elemental concentrations in the crust often do not have a normal distribution and also, if traditional approaches are used to find threshold values, it could result in imprecise recognition of geochemical anomalies (Carranza 2009), Fractal/multifractal models, developed by (Mandelbrot 1983), is extensively used for geochemical exploration, for example, (Turcotte 1986; Cheng et al. 1994; Sim et al. 1999; Li et al. 2003; Qingfei et al. 2008; Zuo et al. 2009; Afzal et al. 2011; Afzal et al. 2013).

----

*Corresponding author.
E-mail address (es): afshinashjaardalan@yahoo.com

These models are more applicable than conventional methods because of considering the spatial relations of data with each other (Cheng et al. 1994; Li et al. 2003; Carranza 2008; Cheng et al. 2011; Afzal et al. 2012; Hassanpour and Afzal 2013; Sadeghi et al. 2012; Heidari et al. 2013; Hosseini et al. 2015). This method's advantages are mostly related to its accuracy as noises are removed from geochemical data (Farahmandfar et al. 2020). The main problem is identification of the geochemical anomalies from the background and separation of the high and extremely geochemical anomalies (Alipour Shahsavari et al. 2020). Various fractal models widely used in geochemical anomalies and mineralized zones, including Concentration–Distance (C–D; Li et al. 2003), Concentration– Number (C–N; Hassanpour and Afzal 2013), Concentration–Perimeter (C–P; Cheng 1995), spectrum-area (S-A; Cheng 1999), Concentration–Volume (C–V; Afzal et al. 2011), and Concentration–Area (C–A; Cheng et al., 1994).

This study aims to use the factor analysis and C-N fractal model for delineation the geochemical anomalies of REEs in granitoids in south of Varcheh 1:100,000 sheet.

2. Methodology

2.1. Concentration-number (C-N) fractal model

The C-N fractal model proposed by Hosseinpour and Afzal (2013) for different background and anomalies separation based on the inverse relationship between their cumulative frequency and concentration, on the basis of N-S model developed by Mandelbrot (1983).

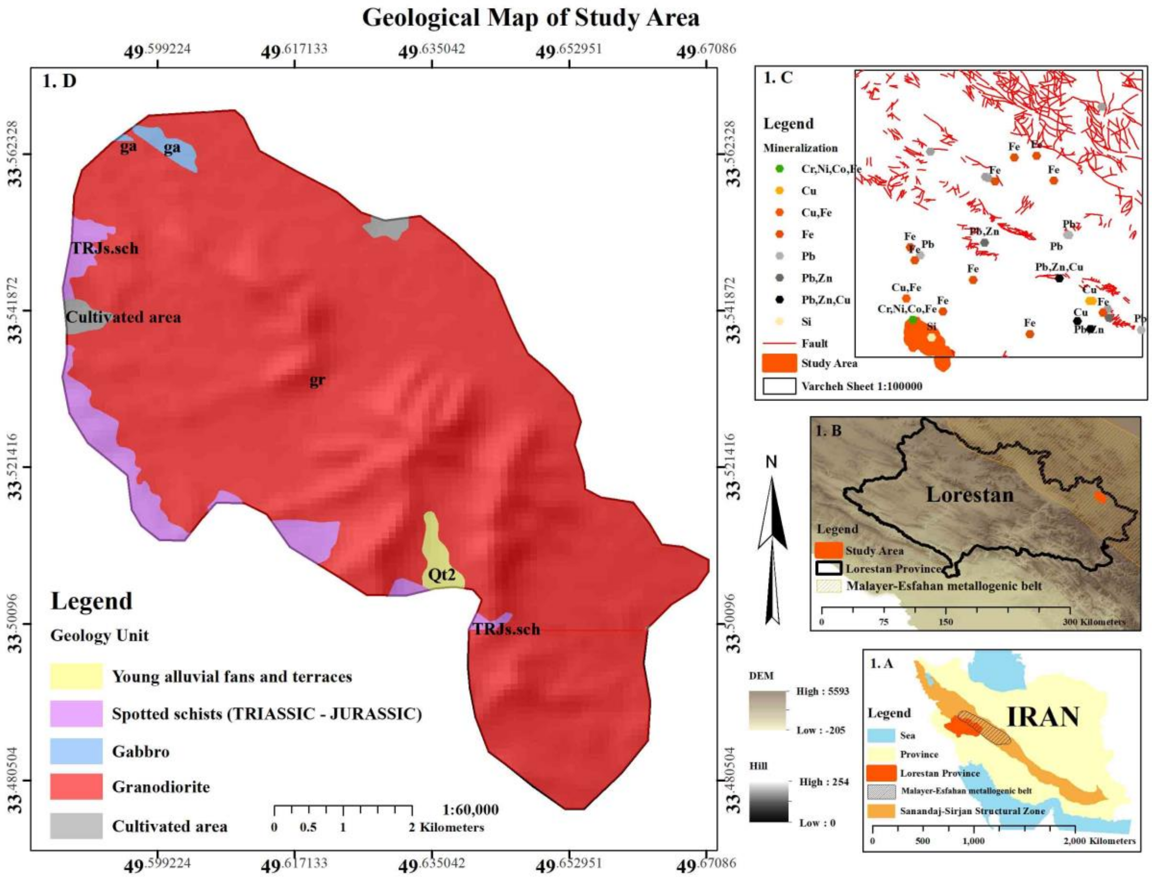

Fig 1. Situation of research area in Iran and simplified geological map

The Number-Size fractal model is a basic approach in various fractal models, which is used to separate natural phenomenon, particularly, in earth science (Kouhestani et al. 2020). The CN model is expressed in equation 1:

$$N(\geq\rho) \propto F\rho^{-\beta} \quad (1)$$

In this equation N (≥ρ) represents the samples' cumulative number with elemental concentration values above or equal to ρ, ρ indicates element concentration, F and β represents a constant, denoting the fractal dimension or scaling exponent of the elemental concentrations distribution. It utilizes raw data with no pretreatment. The C-N log–log plots indicate straight line parts with varying slopes, representing varying concentration ranges (Mandelbrot 1983;Deng et al. 2010; Sadeghi et al. 2012; Hosseini et al. 2015).

2.2. Principal component analysis (PCA) and identification of geochemical anomalies

PCA, as a multivariate analysis instrument, is used for reduction the geochemical data dimensions to smaller factors. Uncorrelated principal components (UPCs) are generated by this analysis based on covariance matrix or correlation (Carranza and Hale 1997; Carranza 2004; Cheng 2007; Muller et al. 2008; Carranza 2008; Ghezelbash et al. 2019). Conventional PCA is a technique that is mostly employed for discovering the internal relationships between elements under analysis via the loadings, which are the correlations between UPCs and elements under analysis (Jolliffe 2002; Carranza 2008; Zuo 2011a; Mahdavi et al. 2015). Moreover, the scores define information between samples collected and UPCs, and this information is employed for generating the multi-element geochemical maps. The eigenvalues calculated for UPCs represent the UPS's variance. Subsequently, it is possible to extract effective UPCs according to the eigenvalues of above 1 (Kaiser 1960; Cheng et al. 2011; Otari and Dabiri 2015). Separation of geochemical anomalies from background has always been an important issue in geochemical projects. In classical methods, anomalies are usually detected only by formulating relationships regardless of the location of each instance. The present research used threshold assessment technique on the basis of standard deviation (S) and median (X) and by following formula:

$$\text{Anomaly} = X+nS$$

Threshold and background can be regarded as X + 2S and median of geochemical data (X). That is, values above X +2S are regarded as anomaly. Values between X + 2S-X + 3S are considered as possible anomaly, and values above X + 3S are regarded as probable anomaly (Webb and Hawkes 1979; Jehangir Khan et al. 2021).

3. Geological setting

The study area, of about 39 km^2, is situated in the Sanandaj-Sirjan (Stöcklin 1968) comprising a part of Malayer-Isfahan metallogenic belt which hosted Pb-Zn mineralization, as well as lots of Fe, Mn, and Barite deposits during the Early Cretaceous.

The characteristics of Sanandaj-Sirjan Zone include the predominant metamorphic rocks and availability of granitoids (Ghaffari et al. 2015; Yazdi et al. 2019). These rocks are made of different metasedimentary aggregations of high to low metamorphic grade. The area's basement includes the pre-Jurassic, low- to highly low-grade metamorphic rocks (Mohajjel 1997; Gharib-Gorgani et al. 2017).

The main unit cropping out in the area is a post-Jurassic plutonic rock composed of granular and porphyry granite, granodiorite, quartz diorite, diorite and gabbro which intruded in Triassic-Jurassic schist (Fig 1). This granitoid is a NW–SE trending structure. Meanwhile, there is an exposure of a quartz diorite-gabbro unit in the northwestern part of this intrusion. Contact metamorphism is well developed in the rocks surrounding the intrusion body. These rocks consist of feldspar, quartz, chlorite, biotite, muscovite, andalusite and sillimanite spots.

4. Material and Methods

A systematic 1 km square grid was used for sampling. Over a total area of about 39 km^2, 59 rock samples, including the granite, granodiorite, diorite and schist were collected (Fig 2). The concentration of 14 REEs (Ce, La, Pr, Nd, Eu, Gd, Sm, Tb, Ho, Dy, Er, Sc, Y, and Yb) was measured by ICP–MS in the laboratory of Iran Mineral Processing Research Center (IMPRC).

5. Discussion

The descriptive statistical parameters for REEs in rock samples of study area are shown in Table 1. The variable's normality was examined by the histograms and box plots (Fig 3). The results show that none of the REEs passed the normality distribution.

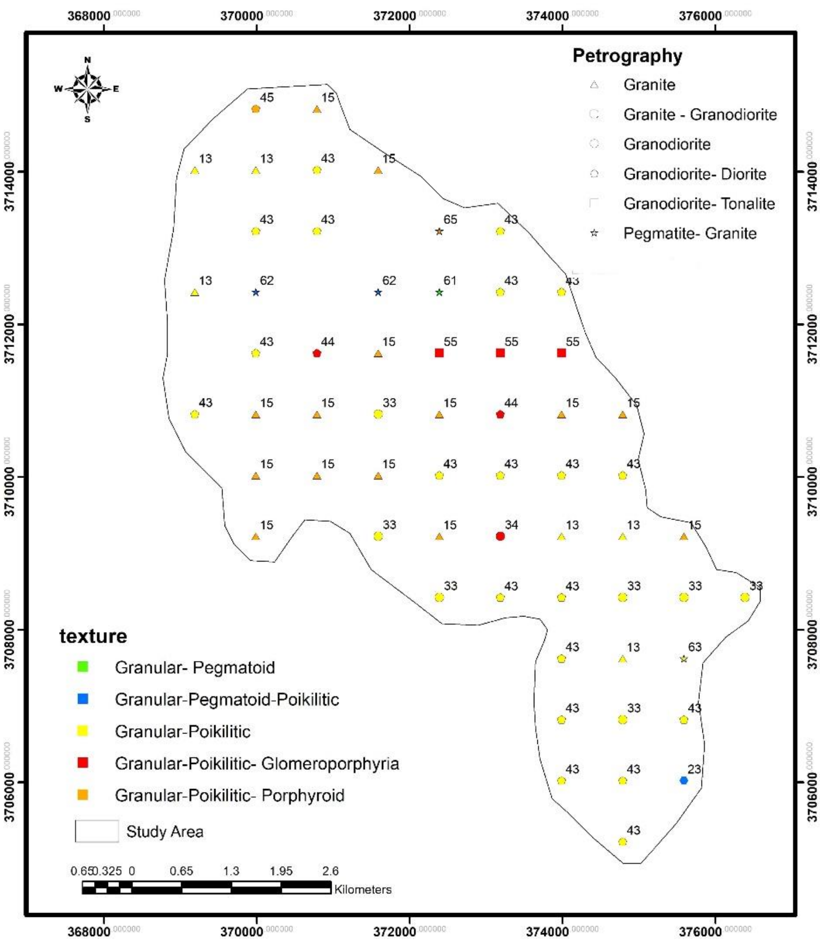

Fig 2. Map of sampling sites, petrography and texture of samples in study area

Table 1. Statistical parameters of REEs concentrations (in ppm) in rock samples from the study area

Statistic parameters	La	Ce	Pr	Nd	Sm	Y
Mean	8.60	17.18	2.46	10.15	1.63	7.02
Median	7.43	14.48	0.75	7.57	0.75	6.08
Std. Deviation	6.78	13.69	5.07	11.60	2.38	3.82
Variance	46.02	187.53	25.69	134.52	5.65	14.63
Skewness	1.99	2.09	2.89	2.64	2.85	1.51
Kurtosis	4.47	4.83	7.07	6.35	6.90	2.59
Minimum	0.22	0.75	0.75	0.31	0.75	1.02
Maximum	33.48	68.02	21.81	53.72	10.48	19.31

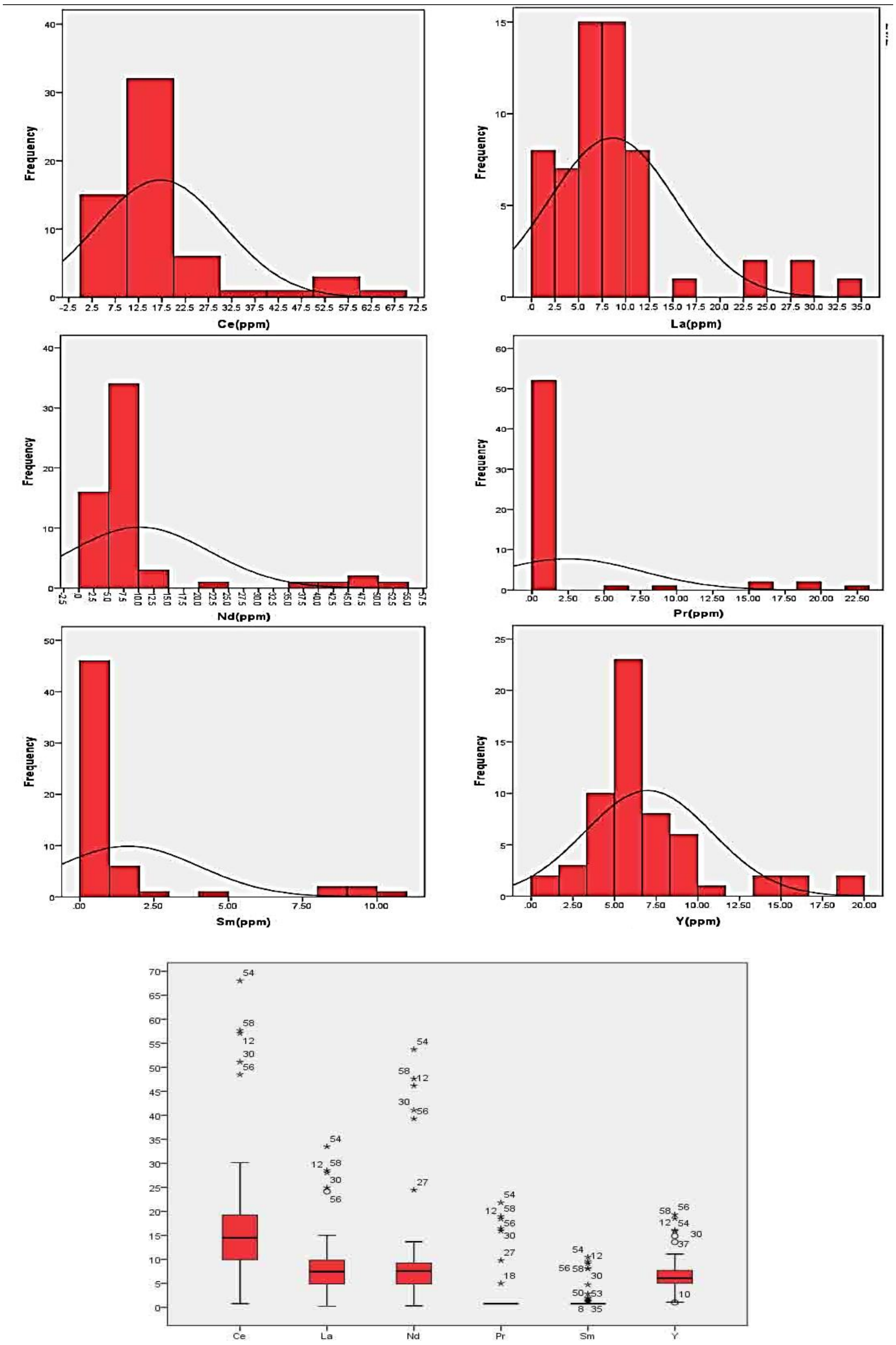

Fig 3. Histogram and box plot of REEs concentration in rock samples of study area (*54= sample number)

Table 2. Thresholds of REEs based on C-N fractal model

Threshold / Elements	Low intensity threshold	Moderate intensity threshold	High intensity threshold	Very high intensity threshold
La	6.31	10	12.59	25.12
Ce	10.47	18.2	23.99	50.12
Pr	5.01		16.22	
Nd	5.01	8.32	10.96	39.81
Sm	1.29		8.32	
Y	7.24	9.33	10.47	14.13

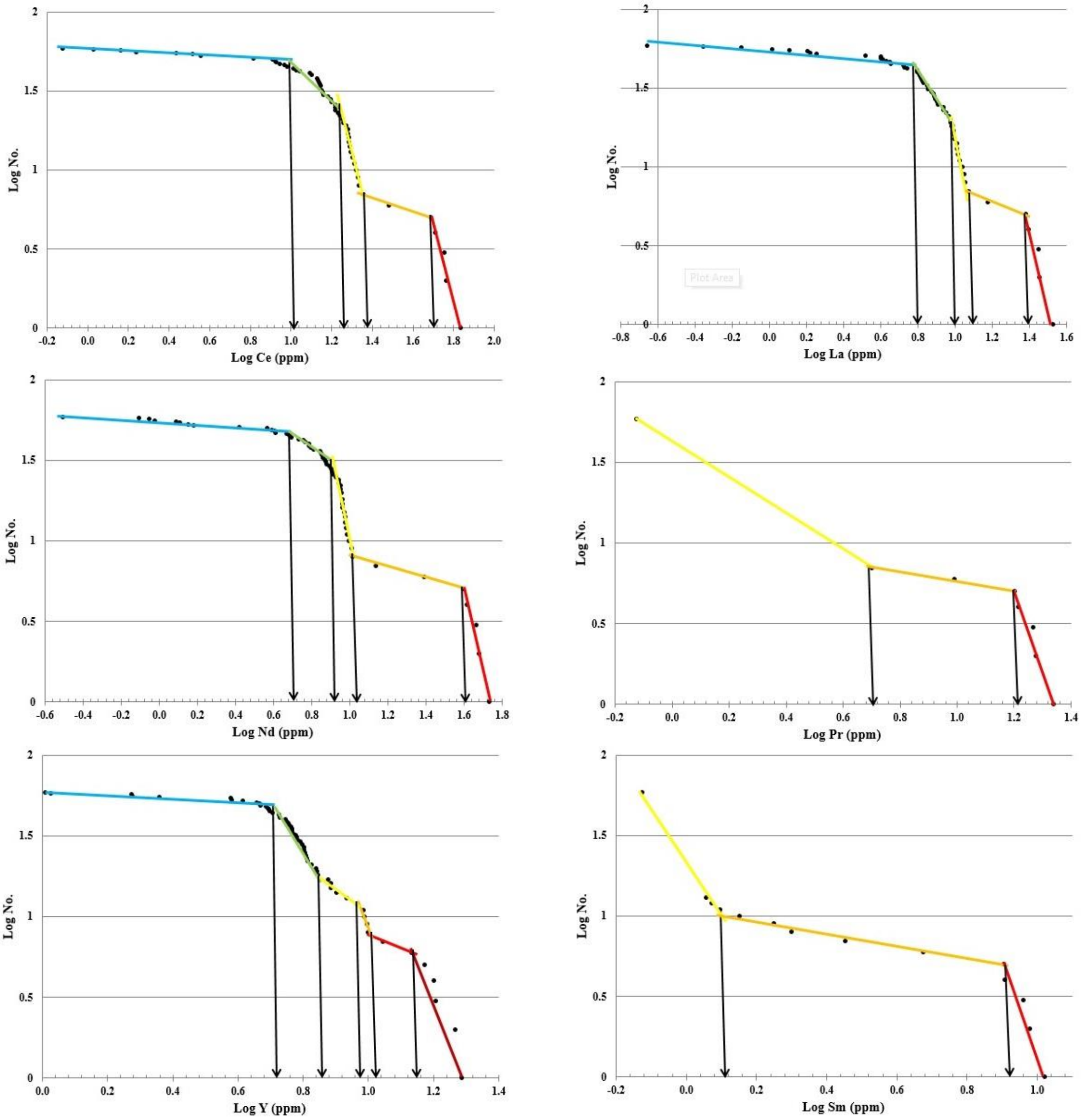

Fig 4. C-N log plots for REEs

5.1. Application of C-N fractal model

According to C-N elemental log-log plots for REEs, three geochemical populations can be identified for Pr and Sm and five geochemical populations for Ce, La, Nd and Y, respectively (Table 2 and Fig 4). The results demonstrate the multifractal nature of REEs in the area. Besides, ArcGIS (10.5) software was used for generating elemental symbol maps (Fig 5). Anomalies of Ce and La with high intensity commence from 50.12 ppm and 25.12 ppm, respectively. The anomalous areas are located in the northern regions of the area, especially in association with schist, granite, granodiorite and quartz diorite.

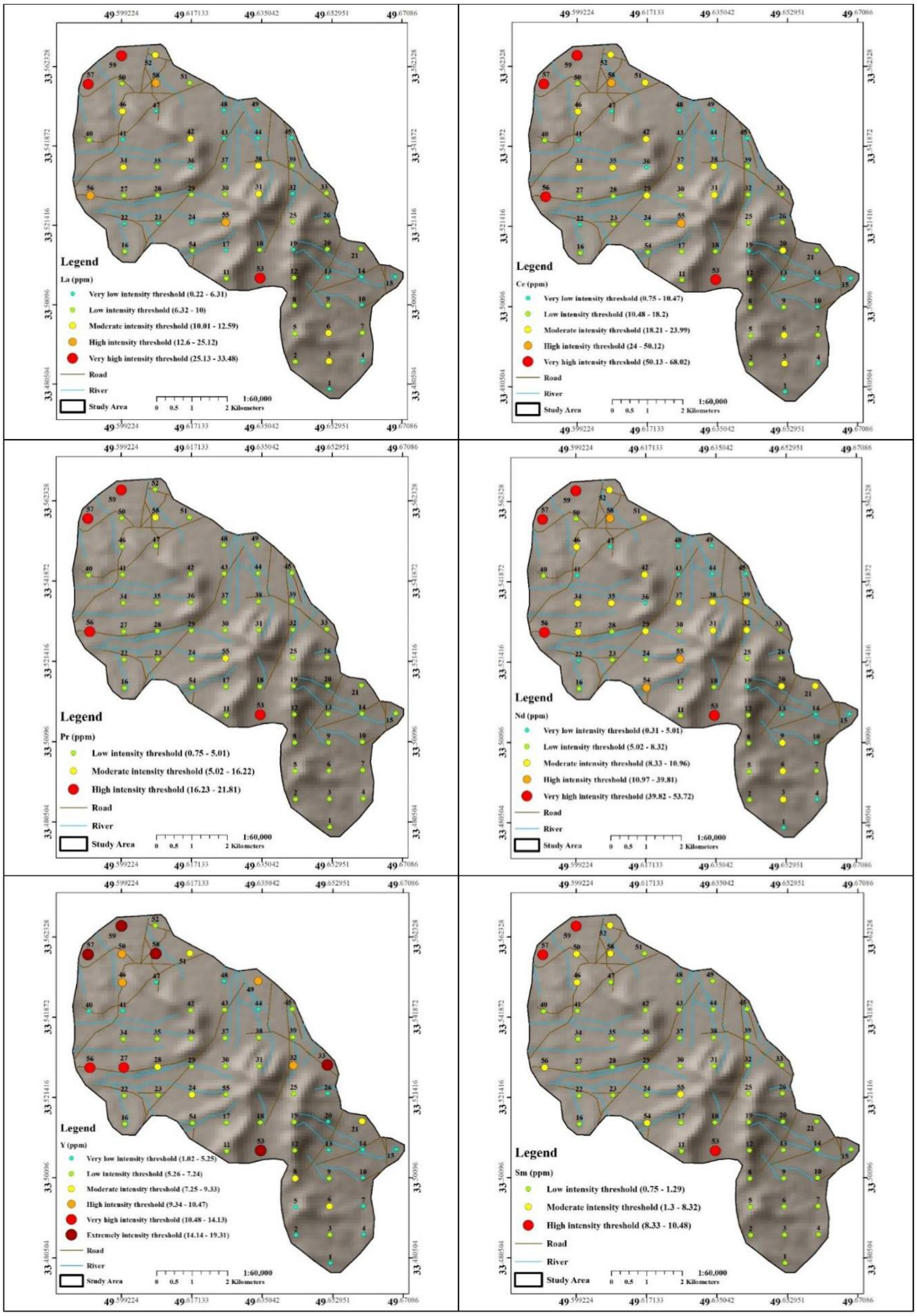

Fig 5. Anomaly Map of REEs based on fractal model.

The main anomalies of Nd show values above 39.81 ppm, which are situated in the central and northern parts consisting of schist, granites, granodiorite and quartz diorite. The main Pr and Sm anomalies, containing values higher than 16.22 ppm and 8.32 ppm, respectively. The anomalous areas are spanned in the southern and northern regions of the area. Finally, high intensive anomalies of Y show values above 14.13 ppm that are scattered in the study area, especially in northern parts.

5.2. Application of PCA and Identification of geochemical anomalies

Primary statistical parameters approach is employed for calculating the Threshold, possible and probable anomalies for REEs (Table 3 and Fig 6).

Table 3. Geochemical anomaly thresholds for REEs in rock samples of study area. X = median value; S = standard deviation.

	La	Ce	Pr	Nd	Sm	Y
Min	0.22	0.75	0.75	0.31	0.75	1.02
X	7.52	14.95	2.46	8.07	1.63	6.81
S	4.32	7.73	5.07	5.23	2.38	1.87
X+S	11.84	22.68	7.53	13.3	4.01	8.67
X+2S	16.17	30.41	12.6	18.53	6.38	10.54
X+3S	20.49	38.14	17.67	23.77	8.76	12.4
Max	33.48	68.02	21.81	53.72	10.48	19.31

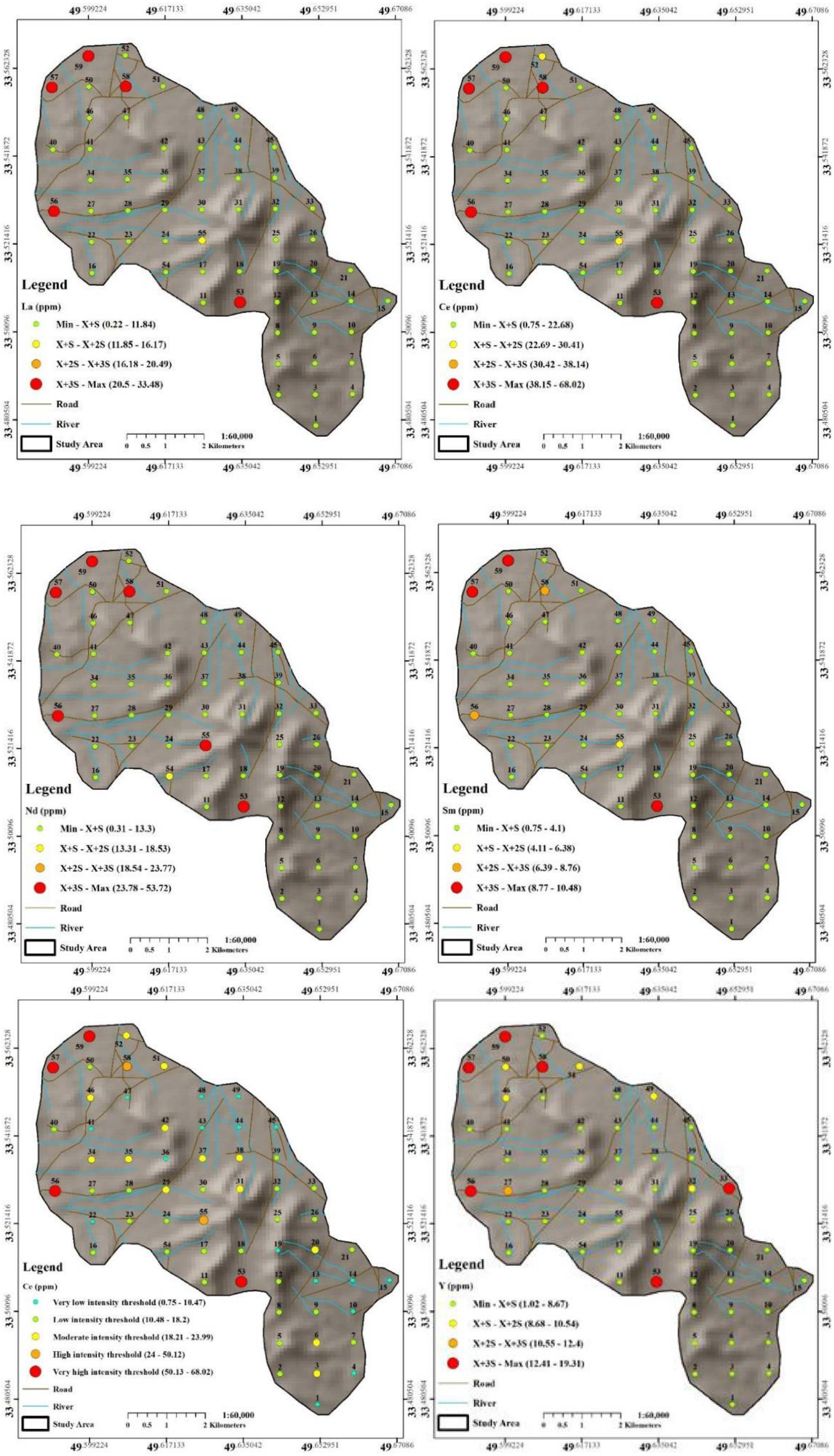

Fig 6. Threshold, probable, and possible anomalies for REEs based on standard deviation (S) and median (X)

The PCA for REEs was used for extracting components that represent geochemical signatures with anomalies in rock samples of study area. 14 elements were combined to produce two significant components (Table 4 and Fig 7).

The variance of the original data set was mostly in the component 1, representing a LREE association composed of Sm, Pr, Eu, Nd, Gd, Tb, Dy, Ce, La, Ho, and Y. Component 2 was characterized by high levels of Er and Yb. Distribution map for indicator factors based on REEs in rock samples is shown in Fig 8. The ratio of LREE/HREE and P content was used to find the origin of REEs in intrusive rocks of the area (Fig 9). The ratio of LREE to HREE in granitoid samples was relatively high. Monazite with a chemical composition of [(Ce, La, Nd, Th) (PO_4, SiO_4)] is a phosphate mineral containing mostly light rare earth elements. REEs are mainly substituted in the structure of monazite. Based on previous studies (Alavi Naeeni 2008; Yazdi et al. 2016), monazite has been frequently observed in heavy mineral samples in report of Varche 100000 sheet. Also, the study of thin sections of the samples shows that minerals of apatite and sphene are also abundant in the Study Area, which can be the source of LREE elements.

Table 4. The highest factor loadings and the corresponding elements for REEs in rock samples

Rotated Component Matrix		
	Component	
	1	2
Pr	**.987**	.054
Sm	**.984**	.085
Nd	**.973**	.163
Eu	**.964**	.089
Gd	**.935**	.293
Ce	**.921**	.221
La	**.913**	.223
Tb	**.901**	.130
Dy	**.862**	.455
Ho	**.862**	.183
Y	**.706**	.687
Sc	.495	.386
Er	-.251	**.891**
Yb	.486	**.715**

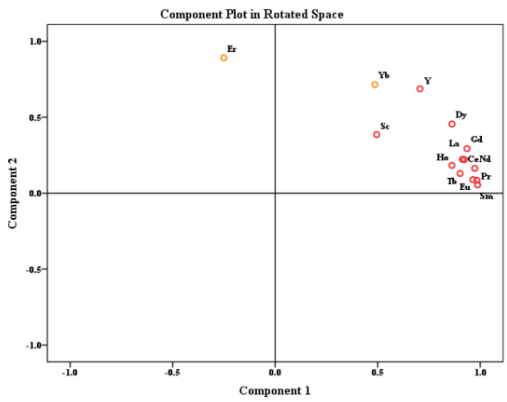

Fig 7. Component plot in rotated space for REEs in rock samples

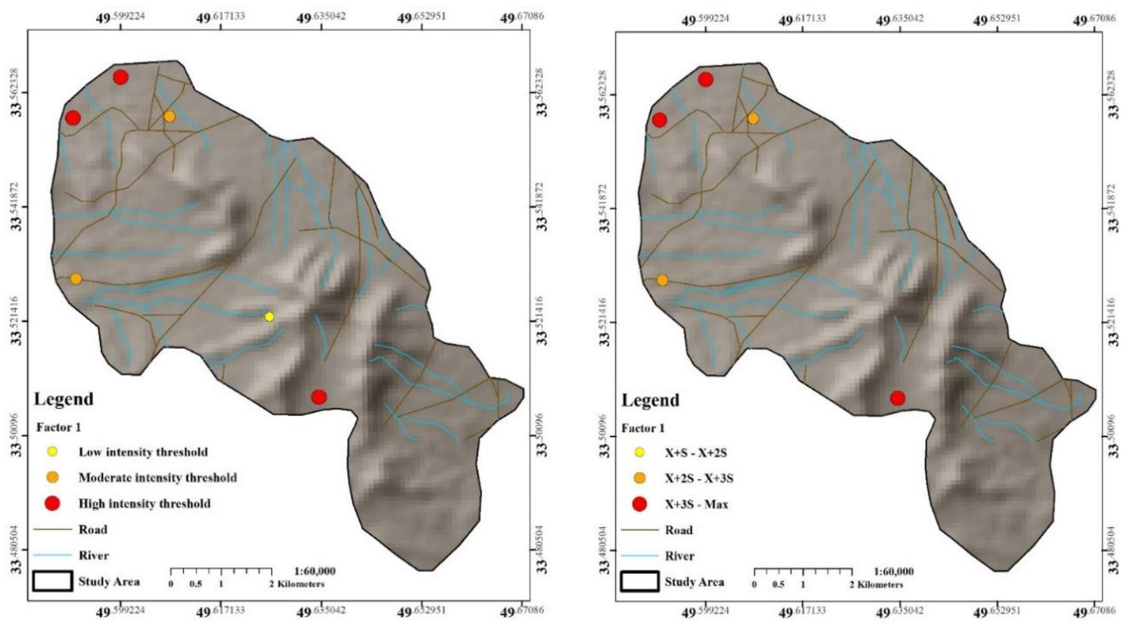

Fig 8. Distribution map for indicator factors based on REEs in rock samples

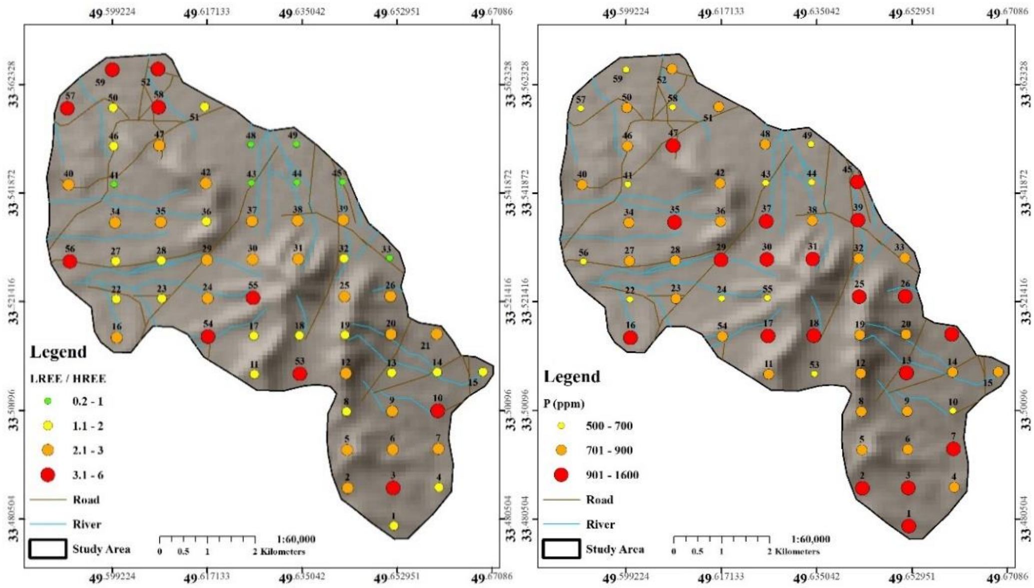

Fig 9. Maps showing the LREE/HREE ratio and P content in rock samples of study area

6. Conclusion

In this study, separation of geochemical anomalies for REEs using C-N fractal model and classical statistics methods yielded to the same results. The classical statistics methods were able to separate three geochemical populations. The results obtained through C-N fractal model exhibited three (Pr and Sm) and five (Ce, La, Nd and Y) anomalies in the northern and western parts of the research area. Finally, the results of this study demonstrated that the integration of the concentration-number fractal model and factor analysis is effective for delineating and recognizing geochemical patterns of rare earth elements in the study area. Based on previous studies, monazite has been frequently observed in heavy mineral samples in study area. Also, the study of thin sections of the samples shows that minerals of apatite and sphene are also abundant, which can be the source of LREE elements. Probable ore deposit in the study area of REE elements associated with complex pegmatite are not far from conceivable. However, further detailed field and petrographic investigations are needed in study areas.

References:

Afzal P, Ahari HD, Omran NR, Aliyari F (2013) Delineation of gold mineralized zones using concentration–volume fractal model in Qolqoleh gold deposit, NW Iran, *Ore Geology Reviews* 55:125-133.

Afzal P, Alghalandis YF, Khakzad A, Moarefvand P, Omran NR (2011) Delineation of mineralization zones in porphyry Cu deposits by fractal concentration–volume modeling, *Journal of Geochemical Exploration* 108:220-232.

Afzal P, Alghalandis YF, Moarefvand P, Omran NR, Haroni HA (2012) Application of power-spectrum–volume fractal method for detecting hypogene, supergene enrichment, leached and barren zones in Kahang Cu porphyry deposit, Central Iran, *Journal of Geochemical Exploration* 112:131-138.

Alavi Naeeni M (2008) Geochemical and heavy mineral exploration in Varcheh 1:100000 sheet, *Geological Survey of Iran, (in Persian)*.

Alipour Shahsavari M, Afzal P, Hekmatnejad A (2020) Identification of geochemical anomalies using fractal and LOLIMOT neuro-fuzzy modeling in Mial area, Central Iran. *Journal of Mining and Environment* 11:99-117.

Arias R, Barona A, Ibarra-Berastegi G, Aranguiz I, Elias A (2012) Assessment of metal contamination in dredged sediments using fractionation and self-organizing maps, *Journal of Hazardous Materials* 151: 78-85.

Asadi S, Moore F, Zaresvandi A (2014) Discriminating productive and barren porphyry copper deposits in the southeastern part of the central Iranian volcano-plutonic belt, Kerman region, Iran: a review. *Earth-Science Reviews* 138: 25-46.

Carranza EJM (2004) Usefulness of stream order to detect stream sediment geochemical anomalies, *Geochemistry: Exploration, Environment, Analysis* 4:341-352.

Carranza EJM (2009) Controls on mineral deposit occurrence inferred from analysis of their spatial pattern and spatial association with geological features, *Ore Geology Reviews* 35: 383–400.

Carranza EJM (2008) Geochemical anomaly and mineral prospectively mapping in GIS. *Handbook of exploration and environmental geochemistry* 11.

Carranza EJM, Hale M (1997) A catchment basin approach to the analysis of reconnaissance geochemical-geological data from Albay Province, Philippines, *Journal of Geochemical Exploration* 60:157-171.

Cheng Q (1999) Spatial and scaling modelling for geochemical anomaly separation, *Journal of Geochemical exploration* 65:175-194.

Cheng Q (2007) Mapping singularities with stream sediment geochemical data for prediction of undiscovered mineral deposits in Gejiu, Yunnan Province, China, *Ore Geology Reviews* 32:314-324.

Cheng Q, Agterberg F, Ballantyne S (1994) The separation of geochemical anomalies from background by fractal methods, *Journal of Geochemical Exploration* 51:109-130.

Cheng Q, Agterberg FP (1995) Multifractal modeling and spatial point processes, *Mathematical Geosciences* 27: 831–845.

Cheng Q, Bonham-Carter G, Wang W, Zhang S, Li W, Qinglin X (2011) A spatially weighted principal component analysis for multi-element geochemical data for mapping locations of felsic intrusions in the Gejiu mineral district of Yunnan, China, *Computers & Geosciences* 37:662-669.

Daneshvar-Saein L (2017) Delineation of enriched zones of Mo, Cu and Re by concentration-volume fractal model in Nowchun Mo-Cu porphyry deposit, SE Iran. *Iranian Journal of Earth Sciences* 9(1): 64–74.

Davis JC, Sampson RJ (2002) Statistics and data analysis in geology vol 33. Wiley New York et al.,

Deng J, Wang Q, Yang L, Wang Y, Gong Q, Liu H (2010) Delineation and explanation of geochemical anomalies using fractal models in the Heqing area, Yunnan Province, China, *Journal of Geochemical Exploration* 105:95-105.

Farahmandfar Z, Jafari M.R, Afzal P, Ashja Ardalan A, (2020) Description of gold and copper anomalies using fractal and stepwise factor analysis according to stream sediments in NW Iran. *Geopersia* 10 :135-148.

Ghaffari M, Rashidnejad-Omran N, Dabiri R, Santos JF, Mata J, Buchs D, McDonald I, Appel P, Garbe-Schönberg D (2015) Interaction between felsic and mafic magmas in the Salmas intrusive complex, Northwestern Iran: Constraints from petrography and geochemistry, *Journal of Asian Earth Sciences* 111: 440-458.

Gharib-Gorgani F, Ashja-Ardalan A, Espahbod MR, Sheikhzakariaee SJ, Yazdi A (2017) Petrology of Mg-bearing Meta Ophiolite Complexes of Qaen-Gazik, Eastern Iran, *National Cave Research and Protection Organization* 4(1).

Ghezelbash R, Maghsoudi A, Daviran M (2019) Prospectivity modeling of porphyry copper deposits: recognition of efficient mono-and multi-element geochemical signatures in the Varzaghan district, NW Iran, *Acta Geochimica* 38:131-144.

Hassanpour S, Afzal P (2013) Application of concentration–number (C–N) multifractal modeling for geochemical anomaly separation in Haftcheshmeh porphyry system, NW Iran, *Arabian Journal of Geosciences* 6:957-970.

Heidari SM, Ghaderi M, Afzal P (2013) Delineating mineralized phases based on lithogeochemical data using multifractal model in Touzlar epithermal Au–Ag (Cu) deposit, NW Iran, *Applied Geochemistry* 31:119-132.

Hosseini SA, Afzal P, Sadeghi B, Sharmad T, Shahrokhi SV, Farhadinejad T (2015) Prospection of Au mineralization based on stream sediments and lithogeochemical data using multifractal modeling in Alut 1: 100,000 sheet, NW Iran, *Arabian Journal of Geosciences* 8:3867-3879.

Jehangir Khan M, Ghazi S, Mehmood M, Yazdi A, Naseem AA, Serwar U, Zaheer A, Ullah H (2021) Sedimentological and provenance analysis of the Cretaceous Moro formation Rakhi Gorge, Eastern Sulaiman Range, Pakistan, *Iranian Journal of Earth Sciences* 13 (4): 251-265.

Jolliffe IT (2002) Principal Component Analysis. Springer, New York.

Kaiser HF (1960) The application of electronic computers to factor analysis, *Educational and psychological measurement* 20:141-151.

Kouhestani H, Ghaderi M, Afzal P, Zaw K (2020) Classification of pyrite types using fractal and stepwise factor analyses in the Chah Zard gold-silver epithermal deposit, central Iran. *Geochemistry: Exploration, Environment, Analysis* 20(4): 496-508.

Li C, Ma T, Shi J (2003) Application of a fractal method relating concentrations and distances for separation of geochemical anomalies from background, *Journal of Geochemical Exploration* 77:167-175.

Mandelbrot BB (1983) The fractal geometry of nature WH Freeman San Francisco USA. WH freeman, San Francisco.

Mohajjel M (1997) Structure and tectonic evolution of Palaeozoic-Mesozoic rocks, Sanandaj-Sirjan zone, western Iran, (PhD Thesis) University of Wollongong.

Muller J, Kylander M, Martinez-Cortizas A, Wüst RA, Weiss D, Blake K, Coles B, Garcia-Sanchez R (2008) The use of principle component analyses in characterising trace and major elemental distribution in a 55 kyr peat deposit in tropical Australia: implications to paleoclimate, *Geochimica et Cosmochimica Acta* 72:449-463.

Otari M, Dabiri R (2015) Geochemical and environmental assessment of heavy metals in soils and sediments of Forumad Chromite mine, NE of Iran, *Journal of Mining and Environmental* 6(2): 251-261.

Pazand K, Hezarkhani A, Ataei M, Ghanbari Y (2011) Application of multifractal modeling technique in systematic geochemical stream sediment survey to identify copper anomalies: a case study from Ahar, Azarbaijan, Northwest Iran, *Chemie der Erde-Geochemistry* 71:397-402.

Qingfei W, Jun D, Li W, Jie Z, Qingjie G, Liqiang Y, Lei Z, Zhijun Z (2008) Multifractal Analysis of Element Distribution in Skarn-type Deposits in the Shizishan

Orefield, Tongling Area, Anhui Province, China, *Acta Geologica Sinica‐English Edition* 82:896-905.

Rantitsch G (2000) Application of fuzzy clusters to quantify lithological background concentrations in stream-sediment geochemistry, *Journal of Geochemical Exploration* 71:73-82.

Sadeghi B, Moarefvand P, Afzal P, Yasrebi AB, Saein LD (2012) Application of fractal models to outline mineralized zones in the Zaghia iron ore deposit, Central Iran, *Journal of Geochemical Exploration* 122:9-19.

Sim B, Agterberg FP, Beaudry C (1999) Determining the cutoff between background and relative base metal smelter contamination levels using multifractal methods, *Computers & Geosciences* 25:1023-1041.

Stöcklin J (1968) Structural History and Tectonics of Iran1: A Review, *AAPG Bulletin* 52:1229-1258.

Turcotte DL (1986) A fractal approach to the relationship between ore grade and tonnage, *Economic Geology* 81:1528-1532.

Webb JS, Hawkes HE (1979) Geochemistry in Mineral Exploration by HE Hawkes and JS Webb. Academic, New York.

Yazdi A, Ashja Ardalan A, Emami MH, Dabiri R, Foudazi M (2019) Magmatic interactions as recorded in plagioclase phenocrysts of quaternary volcanics in SE Bam (SE Iran). *Iranian Journal of Earth Sciences* 11(3):215-25.

Yazdi A, ShahHoseini E, Razavi R (2016) AMS, A method for determining magma flow in Dykes (Case study: Andesite Dyke). *Research Journal of Applied Sciences*11(3): 62-67.

Zuo R (2011a) Decomposing of mixed pattern of arsenic using fractal model in Gangdese belt, Tibet, China, *Applied geochemistry* 26:S271-S273.

Zuo R (2011b) Identifying geochemical anomalies associated with Cu and Pb–Zn skarn mineralization using principal component analysis and spectrum–area fractal modeling in the Gangdese Belt, Tibet (China), *Journal of Geochemical Exploration* 111:13-22.

Zuo R, Cheng Q, Xia Q (2009) Application of fractal models to characterization of vertical distribution of geochemical element concentration, *Journal of Geochemical Exploration* 102:37-43.